

**NASA TECHNICAL
MEMORANDUM**

NASA TM X-52423

NASA TM X-52423

GPO PRICE \$ _____

CSFTI PRICE(S) \$ _____

Hard copy (HC) 300

Microfiche (MF) .65

N 68 - 21233 #653 July 65

FACILITY FORM 602	(ACCESSION NUMBER)	(THRU)
	<u>19</u>	<u>1</u>
	(PAGES)	(CODE)
	<u>TMX-52423</u>	<u>28</u>
	(NASA CR OR TMX OR AD NUMBER)	(CATEGORY)

**BOMBARDMENT THRUSTER INVESTIGATIONS AT
THE LEWIS RESEARCH CENTER**

by Edward A. Richley and William R. Kerslake
Lewis Research Center
Cleveland, Ohio

TECHNICAL PAPER proposed for presentation at
Fourth Joint Propulsion Specialists Conference
sponsored by the American Institute of Aeronautics and Astronautics
Cleveland, Ohio, June 10-14, 1968



NATIONAL AERONAUTICS AND SPACE ADMINISTRATION · WASHINGTON, D.C. · 1968

E-4398

**BOMBARDMENT THRUSTER INVESTIGATIONS AT THE
LEWIS RESEARCH CENTER**

by Edward A. Richley and William R. Kerslake

**Lewis Research Center
Cleveland, Ohio**

**TECHNICAL PAPER proposed for presentation at
Fourth Joint Propulsion Specialists Conference
sponsored by the American Institute of Aeronautics and Astronautics
Cleveland, Ohio, June 10-14, 1968**

NATIONAL AERONAUTICS AND SPACE ADMINISTRATION

BOMBARDMENT THRUSTER INVESTIGATIONS AT THE LEWIS RESEARCH CENTER

Edward A. Richley* and William R. Kerslake**
Lewis Research Center
National Aeronautics and Space Administration
Cleveland, Ohio

Abstract

The current status of various research programs on mercury electron-bombardment thrusters is reviewed. Future thruster requirements as predicted from mission analysis are briefly discussed to establish the relationship with present programs. Thrusters ranging in size from 5 to 150 cm diameter are described. These thrusters have possible near to far term applications extending from station keeping to primary propulsion, respectively. Included is a 5 cm thruster having a power-to-thrust ratio of 220 kW/lb; the 15 cm diameter SERT II thruster; and, a 30 cm thruster designed to produce a 1.5 ampere beam at 2,700 sec specific impulse. Research activities on thruster components are reported in the context of the various thruster programs. These include glass-coated, single accelerator grids that have accumulated more than 500 hr operating time; high-current hollow cathodes of 10 amperes emission; and, a minimum-B discharge chamber.

Introduction

It is generally recognized among members of the electric propulsion community that, with a few exceptions, initial applications of electric propulsion probably will be with systems powered from photovoltaic solar cells. Specific masses of present day solar cell systems indicate that electrostatic thrusters will be required to operate at specific impulses below 5,000 sec in order to minimize overall propulsion system specific mass, estimated to range from 30 to 50 kg/kW. Indications of the potential needs for thrusters capable of high performance at reduced specific impulse can be seen from the values given in table I. Listed are several prospective missions based on studies⁽¹⁻¹²⁾ in which mercury-electron bombardment thrusters were assumed. The compilation is not complete but is only intended to be representative of trends in mission studies reported in the past year or so. The table shows the requirements for thruster operation at less than 5,000 sec. Because of inherent losses, or ion production costs, the efficiency of a bombardment thruster decreases sharply with specific impulse in this region. Thus, continued research is required to ensure optimum performance.

The present mercury electron-bombardment thruster research investigations described herein arose from considerations such as those mentioned above. Discussed first is the 15 cm SERT II thruster. Then the 30, 5, and 150 cm thruster programs will be described. Highlights of research activities on glass-coated accelerators, hollow cathodes, and other thruster components are described in the context of these programs. Finally, performance projections of each of the thrusters are summarized.

* Head, Propulsion Components Section.

** Head, Propulsion Systems Section.

SERT II Thruster

Mission Description

The mission purpose is the demonstration of long life (6 months) space operation of a mercury electron-bombardment ion thruster. The thruster will operate from a space power system (solar cell array) coupled to the thruster by an efficient, "state of the art" power conditioning unit. The SERT II flight is scheduled to be launched in 1969 by a Thorad/Agena booster into an initial 1000-kilometer circular polar orbit. The final spacecraft (Fig. 1) is basically the shell of the second stage Agena on which are mounted two thrusters (nominally 6 mlb thrust each) and a 1.5-kW solar cell array. Attitude control of the solar cells, which must always face the sun, will be maintained by the gravity gradient of the Agena shell and control moment gyros.

Once in orbit, one of the two electric thrusters will be turned on (the other is a redundant system) and the orbit altitude will be gradually changed by the thruster. The orbit change is one measure of thrust. An accelerometer may be used to obtain an additional thrust measurement. A third value of thrust will be calculated from measurements of ion beam current and voltage. The thrust measurement is important not only to evaluate the thruster efficiency, but also to demonstrate the capability of accurate thrust determination, a requirement for future mission trajectory control. Other space experiments to be performed during the mission are: measurement of space plasma and ion beam potentials; measurement of the surface contamination of test sample solar cells located near the thruster; measurement of radio frequency interference noise produced in the ion beam; and measurement of the surface degradation of a test specimen via the changes in optical characteristics.

Thruster Description

The nominal 1 kW thruster system consists of a mercury electron-bombardment thruster with a 15 cm diameter discharge chamber, a mercury plasma-bridge neutralizer, and a pressurized mercury propellant tank. The thruster produces a 0.25-A beam of mercury ions accelerated through a net voltage of 3000 V. This is equivalent to a thrust of 6.2 mlb (= 27.6 mN). A brief description of the thruster operation, which is typical for all the Lewis bombardment thrusters, can be followed with the help of Fig. 2. This figure is a cross-section through the discharge chamber. Liquid mercury propellant is vaporized, passed through an electrical isolator, and enters a distributor manifold. About 20 percent of the main flow passes through the hollow cathode, and the keeper electrode. This initial discharge supplies about 2 amperes of electrons to the main discharge chamber. Eighty percent of the main flow is uniformly injected into the discharge chamber through the distributor holes. A divergent, permanent magnetic field in the discharge chamber helps

trap electrons in the discharge and enhance the ionization process. An iron filing representation of this magnetic field⁽¹³⁾, is shown in Fig. 3. The baffle enhances the ionization process by controlling the flow of electrons between the hollow cathode and the anode. Some ions produced in the discharge chamber drift to the screen and accelerator grids where an applied electric field causes them to accelerate through concentric holes. This beam of positive ions is neutralized downstream of the grids by electrons injected into the beam by the plasma-bridge neutralizer. The neutralizer cathode is identical to the hollow cathode of the main discharge, but requires only one-fourth as much mercury flow. The entire thruster system is surrounded by a ground screen which prevents space plasma electrons from being drawn into the high positive voltage of the thruster surface. A more complete description of the thruster system is found in Ref. 3, and of the discharge chamber characteristics in Ref. 14 and of the plasma-bridge neutralizer in Refs. 15 and 16.

Ground Test Results

Extensive ground testing of the SERT II type thruster has been done in vacuum tanks. This testing has been necessary to establish the reliability and performance of the thruster components. Those that are most subject to erosion are the main cathode, the neutralizer cathode and the accelerator grid. Endurance tests of these components in complete thruster systems began in March, 1967 and are still continuing. The main cathode has had endurance tests up to 2000 hr and the neutralizer cathode up to 3,400 hr. The projected lifetime of the cathode tip area, where the major sputtering erosion occurs, is at least 10,000 hr. The accelerator grid and its mounting insulators have been tested for periods of 3,000 and 3,100 hr and have a projected lifetime of 10,000 hr for most areas of the grid. There is, however, one narrow region at the edge of the accelerator, close to the neutralizer, that has more erosion. This increased erosion is caused by plasma-bridge neutralizer ions falling into the negatively biased accelerator grid. To overcome this problem, grid thickness has been increased in this region.

A fully loaded and operational thruster system has successfully passed vibration testing in 3 axes and random vibration equivalent to booster launch vibration. A thruster system has been assembled on a spacecraft framework and operated in a vacuum tank together with many of the various pieces of "housekeeping" apparatus and auxiliary SERT II experiments.

The performance of the thruster has been optimized from many component tests of the accelerator configurations and the discharge chamber magnetic field shapes⁽¹⁷⁾; hollow cathode and baffle configurations and positions⁽¹⁴⁾; and plasma-bridge neutralizers⁽¹⁶⁾. A 1000-hr endurance test of a prototype thruster system (shown prior to testing in Fig. 4) was completed at the time of this writing (March, 1968). This test was run unattended with a breadboard power conditioning unit. The test was without major incident and measurements of cathode and accelerator grid erosion confirmed previous projected lifetimes. The performance of the thruster is summarized in table II, which contains average values over the 1000-hr period.

Several of the missions given in table I would require 10 or more SERT II size thruster modules. A smaller number of larger size modules would be preferable. For example, a 10 kW system would require only four 2.5 kW thrusters plus, perhaps, one standby as compared to 10 or 11 SERT II thrusters of the 1 kW level. Lower specific impulses are also of interest. On this basis, a 30 cm program was initiated in which the SERT II thruster was scaled up in power level and down in net voltage (i.e., specific impulse). The purpose of the program was (and is) to bring out any critical design problems.

The 30 cm thruster design values chosen are compared in table III with 15 cm SERT II thruster performance values. The thruster input power of 2.1 kW was based on an assumed solar cell output power of 2.5 kW and 0.85 power conditioning efficiency. A photograph of one variation of the thruster that was fabricated is shown in Fig. 5. Overall performance to date has matched or exceeded the design values, however, development of durable flight-worthy components remains to be accomplished. It is significant to note that the initial chamber size was scaled directly from the SERT II dimensions and gave poor performance. Reducing the chamber length by a factor of two (to a length to diameter ratio of 0.37) has resulted in the best performance to date.

Accelerator Grid System

The design ion beam current is six times that of SERT II, while the accelerator area is only increased four times. This poses an accelerator grid design problem. Two designs have undergone preliminary test. The first was a conventionally designed two-grid system having a 74% open area screen grid (SERT II is about 71%). The thruster using this grid system had poor ion chamber performance, 650 eV per beam ion compared to 220 eV/ion for SERT II.

This was attributed to at least two factors. Because of the close grid spacing required to obtain a 1.5 ampere beam (1.25 mm compared with 2.5 mm for SERT II), a center support was incorporated to help maintain a uniform spacing over the 30 cm span. This support projected downstream a few centimeters and probably picked up some direct ion impingement. Another factor was a change in the grid spacing to hole diameter ratio from about 1:1 to about 0.5:1. Ion optics undoubtedly were adversely affected. It should be possible to eliminate both of these problems with improved designs. However, one is still faced with the problems of maintaining satisfactory grid hole alignment and possible thermal warpage.

The second approach was to use a single glass-coated grid, thus eliminating these problems. Single coated grids have been under investigation at Lewis for sometime and early results with 5 cm thrusters are given in Refs. 18 and 19. The concept is compared with a conventional two-grid system in Fig. 6. The insulated glass coating on the accelerator grid is believed to accumulate a surface charge from the plasma in the discharge and take on a potential near plasma potential (approximately equal to the thruster net voltage). The accelerator is biased negatively and ions are extracted by

virtue of the resulting electric field. In the two-grid system, the electric field is established directly between the screen and accelerator grid. Thus the screen grid is eliminated in the glass-coated grid approach. This, of course, also eliminates grid hole alignment problems as well as the problem of maintaining the gap between the grids.

The technique for fabricating the glass-coated grids is described in detail in Refs. 20 and 21. Briefly it consists of spraying a thin layer of a slurry made up of water and powdered Corning #7052 glass onto the molybdenum grid which is made from prepunched sheet. The grid is then furnace fired at about 1200° K in a helium-followed-by-argon atmosphere. This background gas process allows helium bubbles entrained in the glass to diffuse out leaving a virtually bubble-free coating. Successive coatings are applied in this manner to obtain a final coating of the desired thickness. Five coats appear to be adequate (about 0.5 mm maximum thickness) for sustaining 2,000 V. Bench tests show such glass layers capable of withstanding more than 8×10^7 V/m in oil.

Thruster performance with the coated grid shown in Fig. 5 has been excellent. Ion chamber performance of about 180 eV/ion has been attained. Beam divergence characteristics; extended durability, and flight-type mounting assemblies have not yet been thoroughly investigated. Smaller 5 cm diameter coated grids have accumulated more than 200 hr of operation with no deterioration. They have also withstood up to 40 g's of sinusoidal oscillation in the drum mode at the resonant frequency (950 Hz). This is about 4 times as severe a test as the SERT II launch requirements.

A program using a 15 cm SERT II type thruster is underway to investigate suitable mounting methods that will minimize flexure and provide adequate support. One configuration under test is shown in Fig. 7. In this unitized configuration the peripheral mounting assembly is also made of molybdenum. The dished grid is mounted into a notch in one of the assembly rings, then the other assembly ring is joined to it using the final insulating glass coating as a bonding agent. The grid is being tested at a net voltage of 1000 V and with a beam current of about 375 mA. Tests of over 500 hr duration have revealed no major problems.

Hollow Cathode. - A sketch of the SERT II hollow cathode tip (and neutralizer) is shown in Fig. 8. Details of its performance in the SERT II thruster are given in Ref. 14. Tests in the initial 30 cm thruster were conducted using a cathode tip of this design. Tip failures occurred during attempts to obtain from 15 to 20 A emission. (Emission in the SERT II thruster is about 1.75 A and tip temperature is about 1400° K). The higher emission is required because the beam current is a factor of 6 greater in the 30 cm thruster.

A program to reduce tip temperature and increase emission was started. Variations in tip hole size, tip thickness, and number of tip holes are being investigated in bell jar tests. Preliminary results are outlined in Fig. 9. These tests indicate thinner multi-hole tips, or larger single holes, may be the direction to go for lower tip temperature at high emission.

Subsequent improvement in overall thruster design have permitted operation with a conventional SERT II cathode having an enlarged hole. Emission current requirements have been reduced to under 10 A. This is satisfactory for overall thruster evaluation. However, from the durability viewpoint other approaches such as the multi-hole tip may still be required. Although less desirable from a systems viewpoint, multiple cathodes are another possible approach.

Neutralizer. - Hollow-cathode type neutralizers have undergone only preliminary testing thus far in the 30 cm program. The similarity between this type neutralizer and the hollow cathode itself which operates in the much more hostile discharge chamber environment suggests that solving cathode design and durability problems also implies a satisfactory neutralizer. This was true in the SERT II program. Higher coupling voltages might be required in the 30 cm thruster if the neutralizer is located similarly on the periphery of the exhaust beam. If this were to be a serious problem, one solution might be to locate the neutralizer on the thruster axis as suggested in Ref. 22. The neutralizer propellant feed line and electrical lead might be incorporated into the grid stiffening structure using the glass coating techniques described previously.

Other components investigations have not progressed to the point where generalizations can be made. Feed system propellant isolators have not been tested for the 30 cm thruster. Designs of the type developed by Nakanishi⁽²³⁾ may prove adequate. (Fig. 10 is an illustration of the best isolator design reported on in Ref. 23.) Also remaining to be investigated and optimized is the thruster performance during propellant throttling. Propellant throttling by about a factor of two may be required for applications to the outer planets because of the reduction in available solar power at these distances. Of course, the actual throttling range required for a given mission would be a function of the number of thruster modules on board the spacecraft.

Satellite Raising Application

A dramatic illustration of the potentialities of efficient low specific impulse thrusters has been demonstrated in an analysis by Hrach⁽²⁾. In his analysis, the highlights of which are noted here, he compared the payload capabilities of 30 cm vs. 15 cm (SERT II size) thrusters for a Synchronous Equatorial Satellite Mission assuming an SLV-3X/CENTAUR-S booster plus electric stage with 25 kW electric power available. (The powerplant is included in the payload.) The electric stage parameters are given in table IV and the resulting payload capabilities vs. propulsion times are compared in table V. With the larger thruster, propulsion times are significantly reduced by more than 50% with less than 15% reduction in payload capability. The small reduction in payload capability comes about because of additional propellant requirements at the lower specific impulse.

5 CM Thruster

A previous study⁽¹⁹⁾ established the basic possibility of small low voltage bombardment thrusters (less than 500 V net). Such thrusters are attractive in applications such as station keeping that require less than 1 mlb thrust. The

small, low voltage thrusters should permit simplifications and reductions in mass of other system components, particularly power conditioning. In the previous program, the main effort was directed at investigating accelerator grids and at least two promising designs evolved. Continued effort on developing glass-coated grid technology has led to the single-grid concepts described previously herein.

Investigations in the present program are directed at thruster optimization using cathode technology developed in the SERT II program. Table VI lists the present design goals. The values are somewhat arbitrary, but are also conservative, requiring only modest improvements in present day technology to be realized. The current program is aimed at optimizing the propellant introduction mode in conjunction with scaling of the SERT II hollow cathode and related hardware.

Figure 11 is a photograph of an experimental thruster showing the hollow cathode mounted in a mica backplate. This arrangement enables visual observation of the discharge in the pole piece region of the chamber. The view in Fig. 11 is through a glass bell jar mounted to a vacuum facility. The thruster operates through a 12 in. valve into the facility. In the SERT II thruster about 20% of the propellant is introduced into the discharge chamber through the cathode, the remainder being introduced through holes in a distributor backplate via a manifold (see Fig. 2). For the 5 cm thruster, the total propellant flow requirements are about equal to the flow through the SERT II type cathode. For this reason initial designs simply used a SERT II type cathode in the smaller thruster with no other means of propellant introduction. Obviously this would be a highly desirable mode of operation since feed system design is greatly simplified. Although the thruster operated with this design, performance was poor, particularly with respect to propellant utilization. Several innovations have improved performance, among these are an enclosed cathode tip (similar to the enclosed neutralizer reported in Ref. 15) and a slotted cathode pole piece. Power to thrust ratios of about 220 W/mlb have been obtained.

Hollow Cathode and Pole Piece

Performance of the enclosed cathode and the conventional open cathode are compared in Fig. 12. Plotted is keeper voltage as a function of neutral flow through the cathode for a keeper current of 0.5 A. It is evident that not only does the enclosed cathode permit lower keeper voltages, it also extends the cathode operating range to flows less than 15 mA equivalent neutral flow. In tests of 1 to 2 hr duration, thermal stability has been good with no external heat required after start-up.

With the hollow cathode and a conventional cathode pole piece and baffle, ion chamber performance improved by a factor of three when a glass-coated grid was used instead of the conventional two-grid system. Propellant utilization, however, could not be increased above 49 percent, a value well below SERT II performance and well below the 85 percent previously obtained with a thermionic cathode. Because of the differences in propellant introduction modes mentioned above, pole piece variations were investigated. Figure 13 is a photograph of a variable slotted pole piece showing

the rotatable sleeve on the right. Slots are covered with a fine mesh tantalum screen, the object being to contain the plasma in the cathode while at the same time allowing neutral mercury atoms to escape through the slots. Initial tests showed an increase in propellant utilization to 60%.

Magnetic Field Effects

The present experimental thruster uses an electromagnet (see Fig. 11) which is adequate for obtaining performance of the components investigated, but which limits the range of magnetic field shapes available for overall optimization of the discharge chamber. To overcome this difficulty, a thruster has been fabricated with a variable geometry. In addition to a variable ion chamber length, it also has 8 longitudinal mild steel bars individually wound with solenoid coils to permit variation in magnetic field shape and intensity. Although speculative, it is expected that, as was found in the SERT II program, significant improvements in ion chamber performance will be obtained when the magnetic field configuration is optimized.

Thrust Vectoring

Thrust vectoring capabilities remain to be demonstrated. Although mechanical methods may be the most straight forward approach, several alternatives may be possible that would require no moving parts. For example, a variation of a method suggested by Harold R. Kaufman of the Lewis Research Center is illustrated in Fig. 14. The accelerator consists of parallel glass-coated metallic rods. Alternate rods are hooked up in common electrically. All rods operate at an appropriate overall negative bias, but pairs of rods are capable of being biased with respect to each other thus resulting in a vectored exhaust beam. Design of a grid of this type is presently underway using the digital computer method described in Ref. 24.

150 CM Thruster

The 150 cm thruster is designed for power levels in excess of 100 kW, which places its potential applications in the category of primary propulsion for large space vehicles, probably using nuclear-electric power conversion systems. Present investigations of thrusters of this size are exploratory in nature, aimed primarily at seeking general information on scaling effects and identifying major component problem areas.

A brief discussion of this program is included herein mainly for completeness since no additional data has been obtained beyond that reported in Ref. 25. This is partly because the facility was in use for higher priority programs and partly because a major redesign of the thruster was undertaken.

A representative cutaway view of the thruster is shown in Fig. 15. Propellant flows from a distributor manifold into the ion chamber via perforated radial channels located on the chamber rear wall. Ten cathodes are equally spaced on the rear wall and their radial positions may be varied. The ion chamber L/D (length to diameter ratio) is 0.15 and a conventional two-grid accelerator system is used with the exception that it is slightly dished and spacers are used to help maintain uniform grid spacing. Additional details are given in

Ref. 25. Performance highlights reported therein are listed in table VII. Ion chamber performance was poor (900 eV/ion).

An analysis of the chamber performance, when compared with that of smaller thrusters, strongly indicated that the thruster L/D was too small. (As pointed out in Ref. 26, large L/D's may enhance wall recombination losses and short L/D's may enhance direct throughput losses.) As a result of the analysis, a thruster with an L/D of 0.30 has been designed and is presently being fabricated. Another major modification is the re-design of the magnetic field windings and the inclusion of pole pieces to enable divergent magnetic fields to be applied. A drawing of a section of the thruster showing these modifications is presented in Fig. 16.

Supporting Research

The energy required in the discharge chamber to produce a beam ion is about 200 eV/ion in present day optimized thrusters. This represents a factor of 2 to 3 improvement over the past year or so. High percentage open area grids and divergent magnetic fields are the two major factors contributing to these gains. No doubt additional gains will be made in the future, although an increasing degree of sophistication may be required to realize these gains. As an example, one approach presently under investigation is intended to offer some additional insight into basic limitations in the discharge chamber. In this program, the electron transport process across the discharge from the cathode to the anode is being investigated.

Experimentally observed anomalies associated with the electron transport process include the onset of "noise" and a change in slope of the ion production cost curve as the magnetic field is increased beyond a certain value. A theoretical study motivated by these observations is reported in Ref. 27. It includes the calculation of the critical field for the onset of a particular type of instability, and the effect of this instability or plasma oscillation on the ion chamber performance. Similar anomalous diffusion has been widely observed in plasma containment experiments. Some confirmation of the theoretical predictions has been obtained by Cohen⁽²⁸⁾.

From these theoretical ideas, a thruster discharge chamber was designed which should avoid or at least delay the onset of this anomalous diffusion. As shown in Figs. 17(a) and (b), this thruster uses two magnetic field windings. One gives a uniform longitudinal magnetic field, the other is wound in a so-called "Ioffe" or quadrupole configuration, that is, the windings are parallel to the axis of the chamber over a portion of the periphery. (For simplicity, a uniform field is used instead of a divergent field.) This combination has been found to be effective in eliminating the flute instability in magnetic-bottle experiments in the thermonuclear fusion field⁽²⁹⁾. The segmented anode shown in Fig. 17(b) is arranged to minimize interception of the Ioffe magnetic field lines which are circumferential about each set of longitudinal windings. These lines could carry electrons to the anode.

Initial tests have indicated that the configuration is successful in suppressing some of the

instabilities, but the resulting gains in performance appear to be more than offset by the additional magnet power required. Permanent magnet designs for the combined field might be complex and costly. Additional testing to seek simpler, more effective configurations is indicated before consideration of permanent magnet designs.

Program Summary

The status of the various thruster programs can be conveniently summarized and discussed within the framework of a thruster efficiency vs. specific impulse plot as shown in Fig. 18. Shown for comparison are data points from the thrusters, two performance curves from Ref. 30, and an "ideal" curve in which all system losses (including un-ionized propellant) are assumed equal to 200 eV/ion. The curves from Ref. 30 represent present and future performance predictions (as of June 1967) for 1 kW and 2 to 3 kW size thrusters, respectively. All symbols represent data points, except for the 5 cm point which is a design value. The solid symbol is a SERT II prototype thruster system data point and includes all inputs chargeable to the thruster system. In short, it is the most complete "state-of-the-art" thruster system point.

The 150 cm data point falls far below the ideal curve, showing that further improvement may be expected in that program. Performance improvements up to the level of the ideal curve may be difficult to attain. The 1 kW curve level, however, seems to be a reasonable interim goal for this size thruster, particularly at lower specific impulses.

The 5 cm design goal is conservative, falling on an extension of the < 1 kW curve. Performance in excess of 15% efficiency has been obtained with non-optimized thrusters. Of more significance to this size thruster is the power-to-thrust ratio and thrust vectoring capability. Values of power-to-thrust of 220 W/mlb have been obtained, putting this thruster well within the present range of interest. Thrust vectoring capability remains to be demonstrated.

As mentioned earlier, a 15 cm SERT II type thruster is being used to evaluate prospective glass-coated accelerator grid designs for the 30 cm program. The data point on Fig. 18 is of interest, though, both because it demonstrates the validity of the 1 kW curve and because it provides a comparison point for the 30 cm data.

The 30 cm thruster data points illustrate the important point that certain losses are fixed, or at least do not scale directly with size and power level. The data points shown exceed the future predicted curve of Ref. 30. These data should be viewed conservatively since long life has not been demonstrated. (Data taken at the Jet Propulsion Laboratory with 20 cm thrusters have also matched or exceeded this curve⁽³¹⁾.) The Lewis thrusters are not optimized for maximum efficiency. Optimization would lead to further improvement which might compensate for the effects of including any changes required to attain long life. In view of this, it seems reasonable to regard the 1967 "future" curve of Ref. 30 as the 1968 "present" curve for thruster systems of the 2 to 3 kW level.

These large improvements over a short period

of time could justify a prediction that, for thruster systems of 2 to 3 kW, the performance levels represented by the "ideal" curve may be achieved within a few years--say by 1972. In the context of the needs indicated in table I, bombardment thrusters capable of fulfilling a wide variety of applications are rapidly becoming available.

References

1. Godwin, R. C. and Rees, T., "Electric Propulsion for Eldo Vehicles," Paper presented at the British Interplanetary Society, Technical Meeting on Research and Development in Propulsion Technology, London, England, Oct. 31 - Nov. 1, 1967.
2. Hrach, F., Unpublished Analysis, National Aeronautics and Space Administration, Cleveland, Ohio.
3. Kerslake, W. R., Byers, D. C., and Staggs, J. F., "SERT II Experimental Thruster System," Paper 67-700, Sept. 1967, AIAA, New York, N.Y.
4. Meissinger, H. F. and Greenstadt, E. W., "Use of Electric Propulsion for Exploring the Distant Regions of the Geomagnetic Tail," Paper 68-120, Jan. 1968, AIAA, New York, N.Y.
5. Wood, L. H., Dailey, C. C., Katz, L., and Vachon, R. I., "Planetary Photographic Exploration with Solar-Electric Propulsion," Paper 67-712, Sept. 1967, AIAA, New York, N.Y.
6. Moliter, J. H. and Olson, R. N., "Solar-Electric Propulsion Systems for Unmanned Space Missions," Paper 67-713, Sept. 1967, AIAA, New York, N.Y.
7. Meissinger, H. F., Park, R. A., and Hunter, H. M., "A 3 KW Solar-Electric Spacecraft for Multiple Interplanetary Missions," Paper 67-711, Sept. 1967, AIAA, New York, N.Y.
8. Strack, W. C. and Zola, C. L., "Solar-Electric Propulsion Probes for Exploring the Solar System," TM X-52318, 1967, National Aeronautics and Space Administration, Cleveland, Ohio.
9. Zola, C. L., "Jovian Planet Missions for Solar Cell Powered Electric Propulsion Spacecraft," Paper 68-118, Jan. 1968, AIAA, New York, N.Y.
10. Sauer, C. G., Jr., "Trajectory Analysis and Optimization of a Low-Thrust Solar Electric Jupiter Flyby Mission," Paper 67-710, Sept. 1967, AIAA, New York, N.Y.
11. Flandro, G. A., "Solar Electric Low Thrust Missions to Jupiter with Swingby Continuation to the Outer Planets," Paper 68-117, Jan. 1968, AIAA, New York, N.Y.
12. Park, R. A., Bailey, W. Dickerson, W. D., and Smith, D. B., "Solar Electric Propulsion Mission to the Comets," Paper presented at The Regional Symposium on Planetary Geology and Geophysics of the American Astronautical Society, Boston, Mass., May 25 - 27, 1967.
13. Knauer, W. and Poeschel, R., "Discharge Chamber Studies for Mercury Bombardment Ion Thrusters," NASA CR-72350, 1968, Hughes Research Laboratories, Malibu, Calif.
14. Bechtel, R. T., Csiky, G. A., and Byers, D. C., "Performance of a 15-Centimeter Diameter, Hollow-Cathode Kaufman Thruster," Paper 68-88, Jan. 1968, AIAA, New York, N.Y.
15. Hall, D. F., Kemp, R. F., and Shelton, H., "Mercury Discharge Devices and Technology," Paper 67-669, Sept. 1967, AIAA, New York, N.Y.
16. Rawlin, V. K. and Pawlik, E. V., "A Mercury Plasma-Bridge Neutralizer," Paper 67-670, Sept. 1967, AIAA, New York, N.Y.
17. Bechtel, R. T., "Discharge Chamber Optimization of the SERT II Thruster," Paper 67-668, Sept. 1967, AIAA, New York, N.Y.
18. Margosian, P., "Preliminary Tests of Insulated Accelerator Grid for Electron-Bombardment Ion Thruster," TM X-1342, 1967, National Aeronautics and Space Administration, Cleveland, Ohio.
19. Nakanishi, S., Richley, E. A.; and Banks, B. A., "High Perveance Accelerator Grids for Low Voltage Kaufman Thrusters," Paper 67-680, Sept. 1967, AIAA, New York, N.Y.
20. Banks, B. A., "Composite Ion Accelerator Grids," Paper presented at the Third International Conference on Electron and Ion Beams in Science and Technology, Boston, Mass., May 6 - 9, 1968.
21. Banks, B. A., "A Bubble Reduction Process for Glass Coatings on Electron-Bombardment Ion Thruster Grids," Proposed Technical Note, National Aeronautics and Space Administration, Cleveland, Ohio.
22. Banks, B. A., and Richley, E. A., "Radially Slotted Grids for a Kaufman Ion Thruster," Journal of Spacecraft and Rockets, vol. 4, No. 11, Nov. 1967, pp. 1562-1563.
23. Nakanishi, S., "Experimental Investigation of Mercury Propellant Feed Isolators for Kaufman Thrusters," Proposed Technical Memorandum, National Aeronautics and Space Administration, Cleveland, Ohio.
24. Lathem, W. C. and Staggs, J. F., "A Divergent-Flow Contact-Ionization Electrostatic Thruster For Satellite Attitude Control Or Station Keeping," TN D-4420, 1968, National Aeronautics and Space Administration, Cleveland, Ohio.
25. Nakanishi, S., "Experimental Investigation of A 1.5 Meter Diameter Kaufman Thruster," Paper 67-725, Sept. 1967, AIAA, New York, N.Y.
26. Richley, E. A. and Mickelsen, W. R., "Effects Of Molecular Flow In Plasma Generation And Some Analyses of Space Charge Flow In Ion Acceleration," Paper 64-7, Jan. 1964, AIAA, New York, N. Y.

27. Cohen, A. J., "Onset of Anomalous Diffusion In Electron-Bombardment Ion Thruster," TN D-3731, Nov. 1966, National Aeronautics and Space Administration, Cleveland, Ohio.
28. Cohen, A. J., "Anomalous Diffusion In A Plasma Formed From The Exhaust Beam Of An Electron-Bombardment Ion Thruster," Proposed Technical Note, National Aeronautics and Space Administration, Cleveland, Ohio.
29. Gott, Yu. V., Ioffe, M. S., and Telkovsky, V. G., "Some New Results on Confinement in Magnetic Traps," Nuclear Fusion Supplement, Part III, 1962, pp. 1045-1047.
30. Kerrisk, D. J. and Kaufman, H. R., "Electric Propulsion Systems For Primary Spacecraft Propulsion," Paper 67-424, June 1967, AIAA, New York, N.Y.
31. Masek, T. D. and Pawlik, E. V., "Thrust System Technology For Solar Electric Propulsion," Paper 68-541, June 1968, AIAA, New York, N.Y.

Mission Class	Power Level Range (at 1 A.U.), kW	Specific Impulse Range, sec	Thruster Efficiency Range	Reference
EARTH ORIENTED SERT II Geomagnetic Tail Satellite Raising	1 2 - 3 7 - 25	1900 - 5000	0.40 - 0.70	1, 2, 3, 4
INNER PLANETS (Mars orbiter, Solar monitor, Solar probe)	3 - 10	4000 - 5000	.60 - .70	5, 6, 7, 8
OUTER PLANETS (Jupiter flyby, Grand tour)	10 - 17	3000 - 4500	.60 - .70	6, 8, 9, 10, 11
OTHER (Asteroid belt, Out of ecliptic, Comet probe)	2 - 3.5	4000 - 5000	.57 - .67	4, 12

TABLE I. - PROSPECTIVE SOLAR-ELECTRIC PROPULSION MISSIONS FOR MERCURY ELECTRON-BOMBARDMENT THRUSTERS

POWER:	
Main Vaporizer (2.1 gm/hr, or 0.284 A flow)	7 W
Cathode	
Heater, 15 W	24 W
Keeper, 3 W (10 V, 0.3 A)	
Isolator heater, .6 W	
Discharge (36 V)	
220 eV/ion at 88% utilization	55 W
Accelerator (~2000 V)	4 W
Neutralizer (0.012 A flow)	127 W
Vaporizer, 4 W	
Tip heater, 15 W	
Keeper, (22 V) 4 W	
Coupling (15 V) 4 W	
Ion Beam (0.25 A)	750 W
Overall power efficiency, percent	86
Overall propellant efficiency, percent	85
Thruster efficiency	73
Thrust (calculated)	6.2 mlb (27.6 mN)
Effective specific impulse	4650 sec
Mass of thruster system (exclude gimbals and propellant)	8 kg
Mass of thruster and neutralizer only	3 kg

TABLE II. - SERT II THRUSTER SYSTEM PERFORMANCE.

Parameter	30 cm Design	SERT II Performance
Input power, kW	2.1	0.87
Net voltage, V	1000	3000
Beam current, A	1.5	0.25
Utilization efficiency, percent	85	85
Overall efficiency, percent	60	73
Thrust	22 mlb (98 mN)	6.2 mlb (27.6 mN)
Effective specific impulse, sec	2750	4650

TABLE III. - THRUSTER COMPARISON

Parameter	Thruster size	
	15 cm	30 cm
Thruster efficiency*, percent	57	49
Specific impulse, sec	4650	1900
Thruster and tankage mass, kg	255	176
Other system mass, kg	118	106
Number of thrusters	25	20

*Includes power conditioning efficiency of 88%.

TABLE IV. - ELECTRIC STAGE PARAMETER COMPARISON
FOR A SYNCHRONOUS SATELLITE RAISING MISSION,
SLV-3X/CENTAUR-S BOOSTER AND 25 kW
POWER ASSUMED(2)

Initial circular orbit, n. mi.	15 cm		30 cm	
	Propulsion time, days	Gross payload, kg	Propulsion time, days	Gross payload, kg
1000	400	3760	178	3220
2000	288	2980	127	2630
4000	180	2080	78	1920
8000	100	1340	46	1270

TABLE V. - RESULTS OF SATELLITE RAISING MISSION ANALYSIS FOR THRUSTERS OF TABLE IV(2)

Input power, W	54
Net voltage, V	400
Beam current, mA	32
Utilization efficiency, percent	85
Overall efficiency, percent	20
Thrust	0.3 mlb (1.33 mN)
Effective specific impulse, sec	1700
Power to thrust ratio, W/mlb	180

TABLE VI. - 5 CM THRUSTER DESIGN VALUES

Input power, kW	130
Net voltage, V	8900
Beam current, A	16
Utilization efficiency, percent	87
Overall efficiency, percent	70
Thrust	0.5 lb (2.22 N)
Effective specific impulse, sec	8200

TABLE VII. - 150 CM THRUSTER PERFORMANCE VALUES

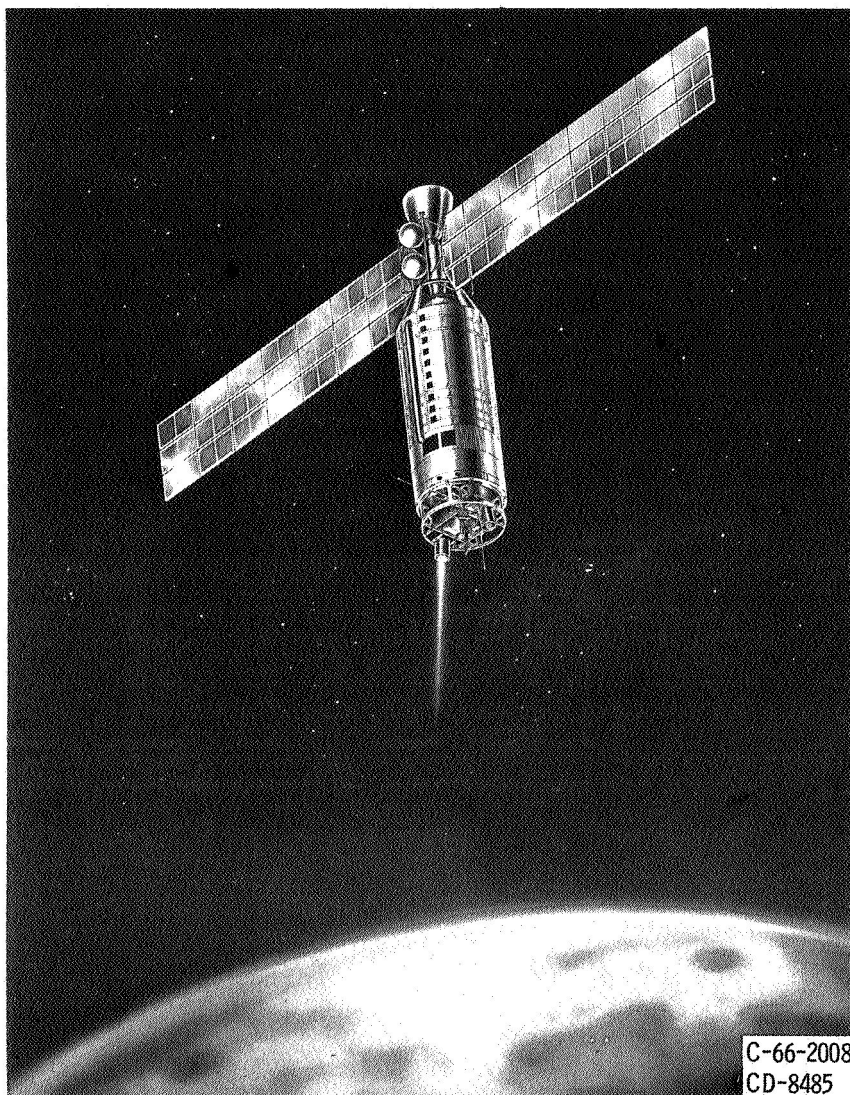


Figure 1. - Artist's drawing of SERT II spacecraft and solar-cell array in orbit.

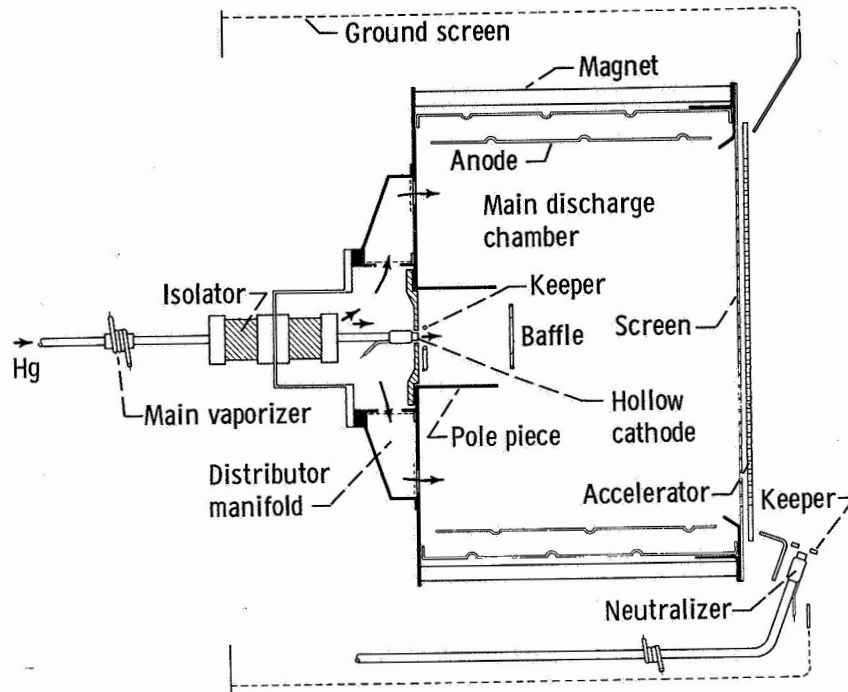


Figure 2. - Section view of SERT II thruster.

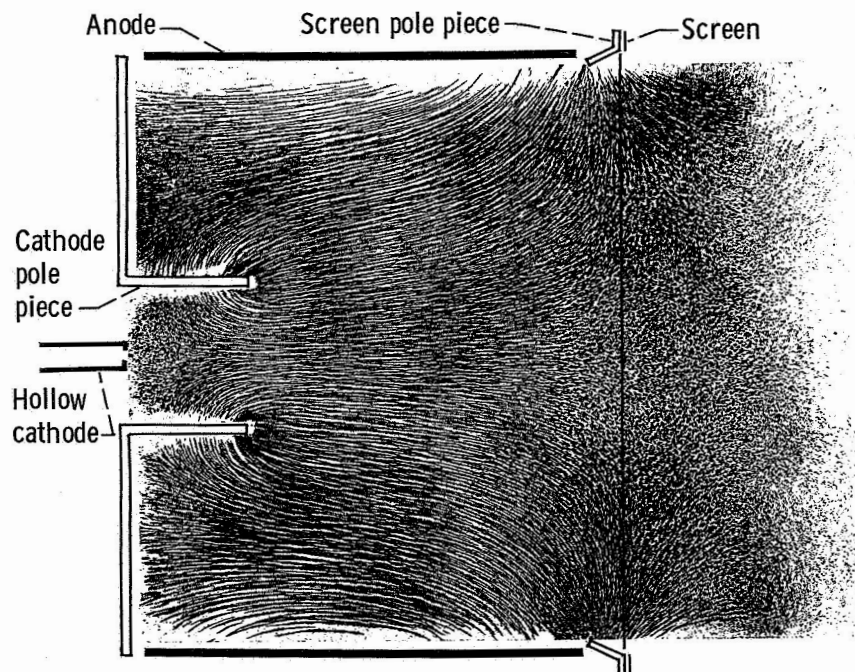


Figure 3. - Powered-iron magnetic-field map of the SERT II thruster (Ref. 13).

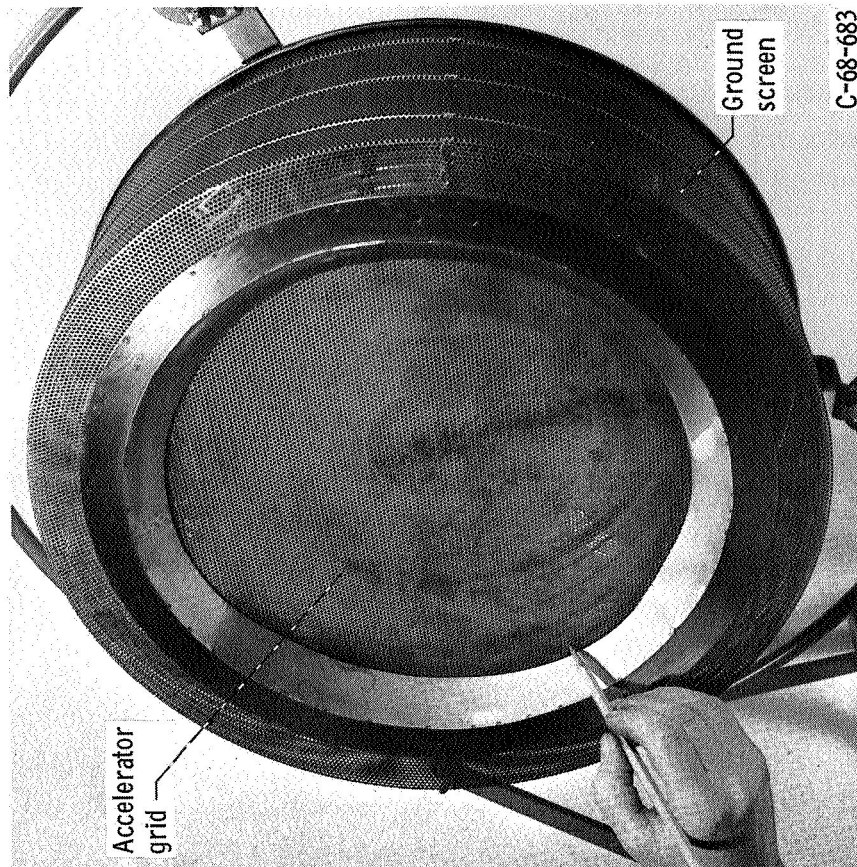


Figure 5. - 30 cm thruster with glass-coated accelerator grid.

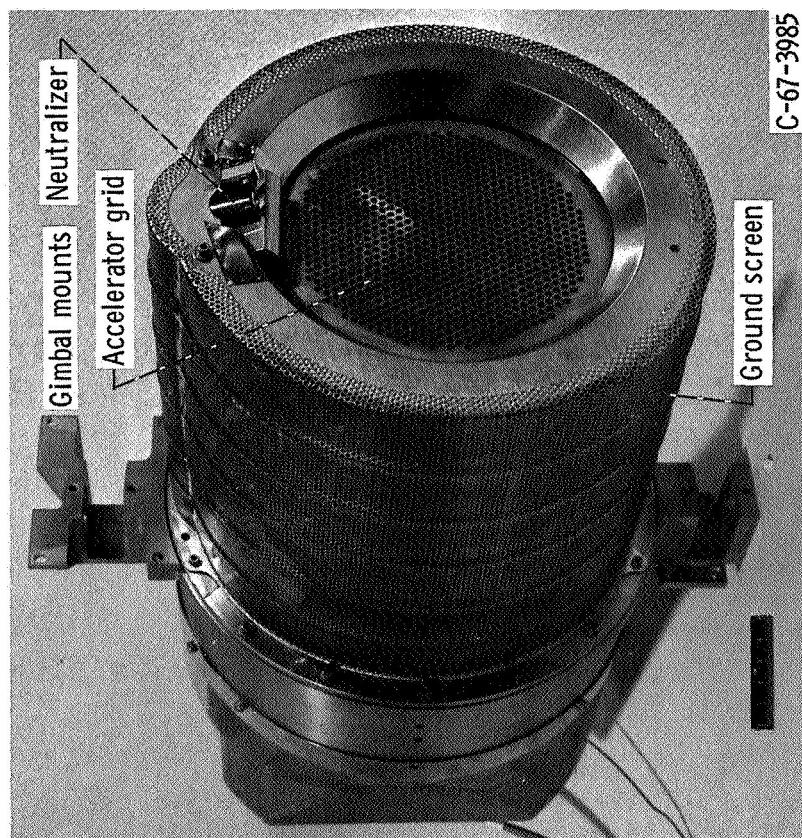


Figure 4. - SERT II prototype thruster system.

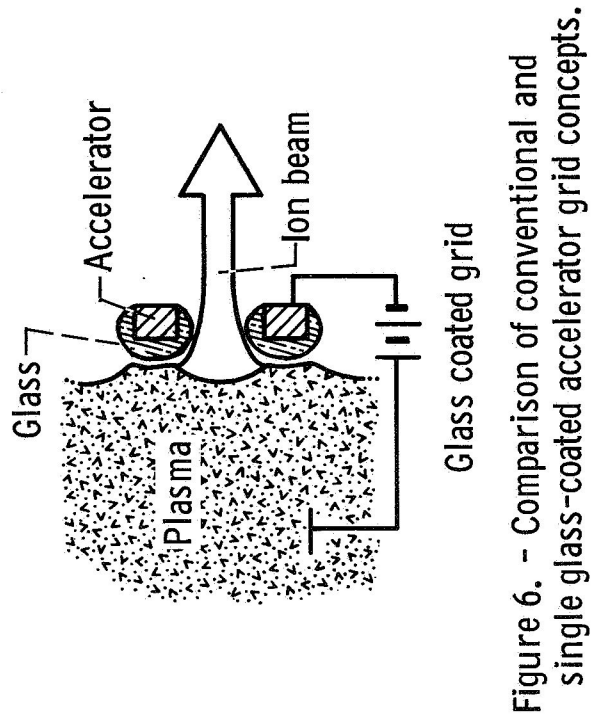
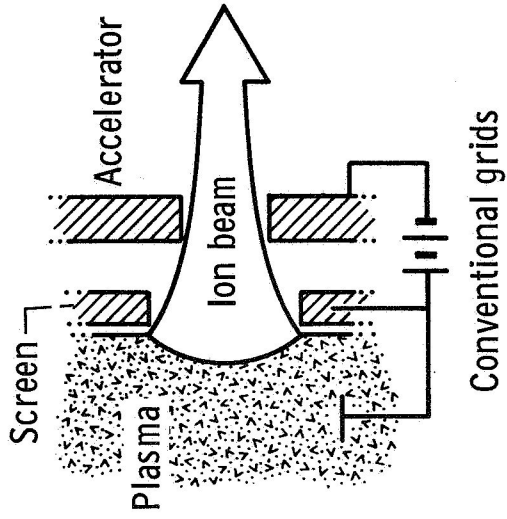


Figure 6. - Comparison of conventional and single glass-coated accelerator grid concepts.

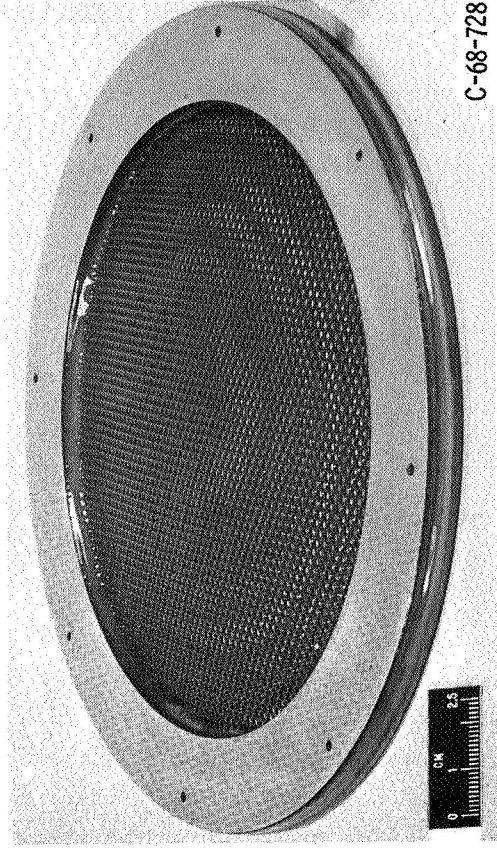


Figure 7. - 15 cm glass-coated grid with unitized mounting ring.

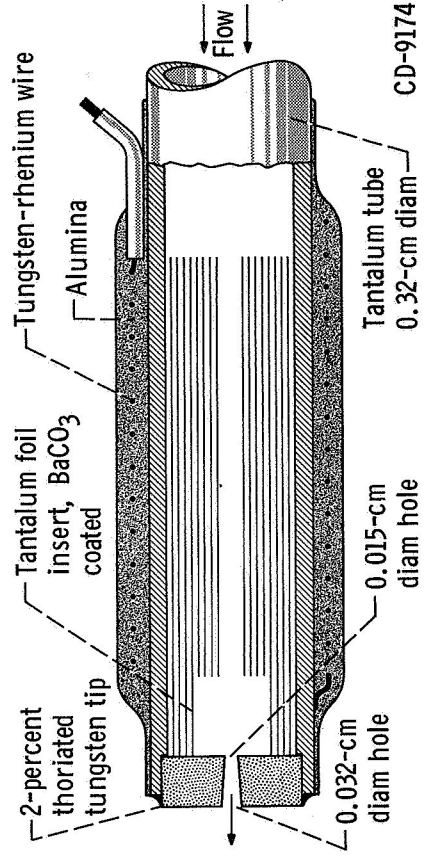


Figure 8. - Sketch of SERT II type hollow cathode and neutralizer.

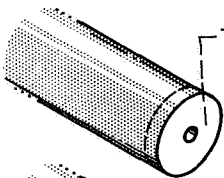
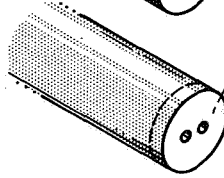
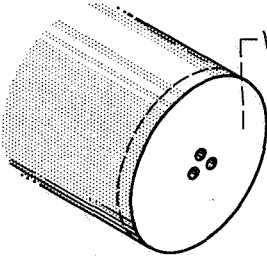
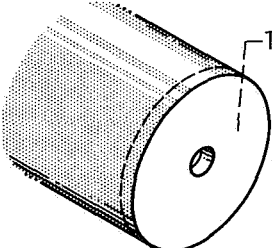
Configuration	Tip thickness, mm	Tip diameter, mm	Hole diameter, mm	Temperature, °K
 Th-W	1.0	3.1	0.4	2083
 Mo	0.75	3.1	0.175	1773
 W	0.50	6.25	0.175	1693
 Th-W	0.50	6.25	0.75	1323

Figure 9. - Operating tip temperatures for various cathodes at 10 amperes emission.

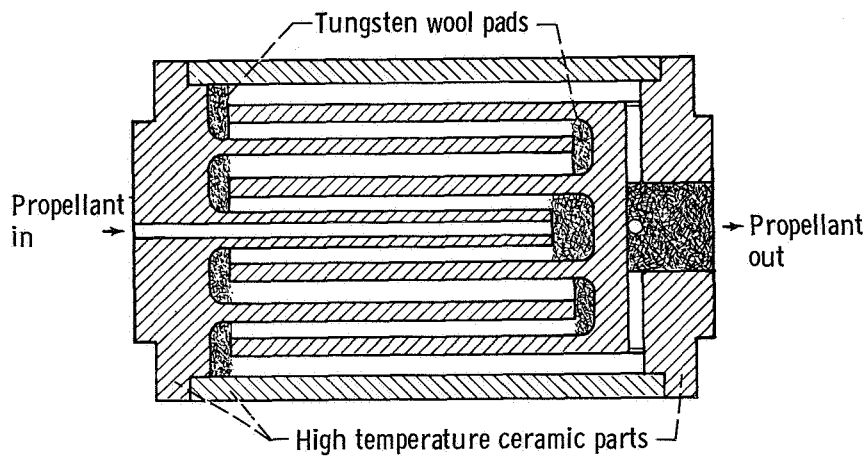


Figure 10. - Sketch of mercury propellant feed isolator (Ref 23). Minimum breakdown voltage, 4 400 v, for mercury flows up to 100 mA equivalent current. Maximum steady state leakage current 0.02 mA at 5 000 v.

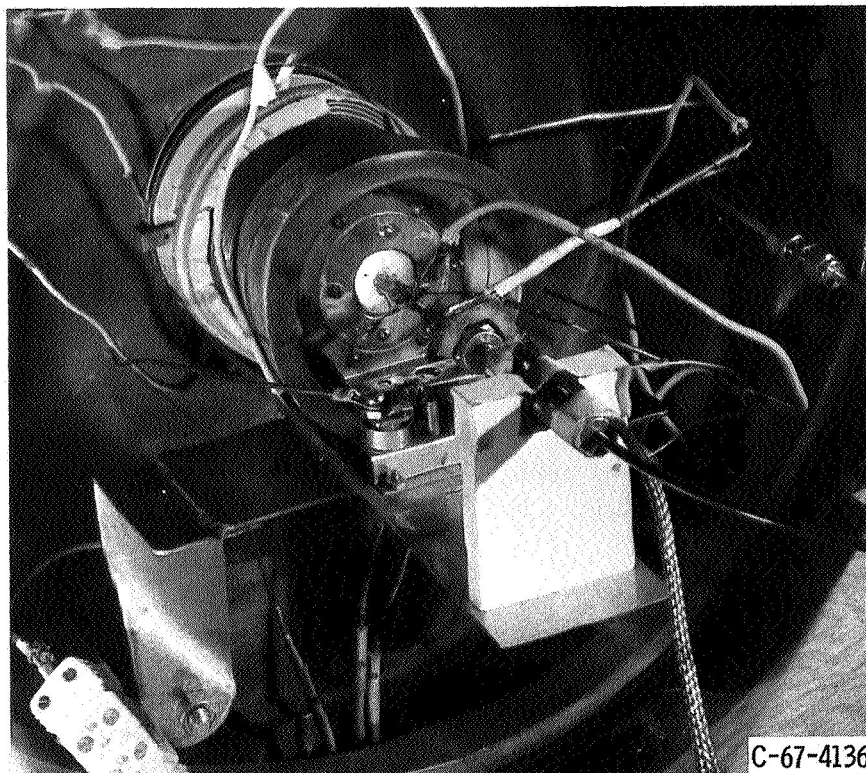


Figure 11. - Experimental 5 cm hollow-cathode thruster in operation. Viewed through glass bell jar.

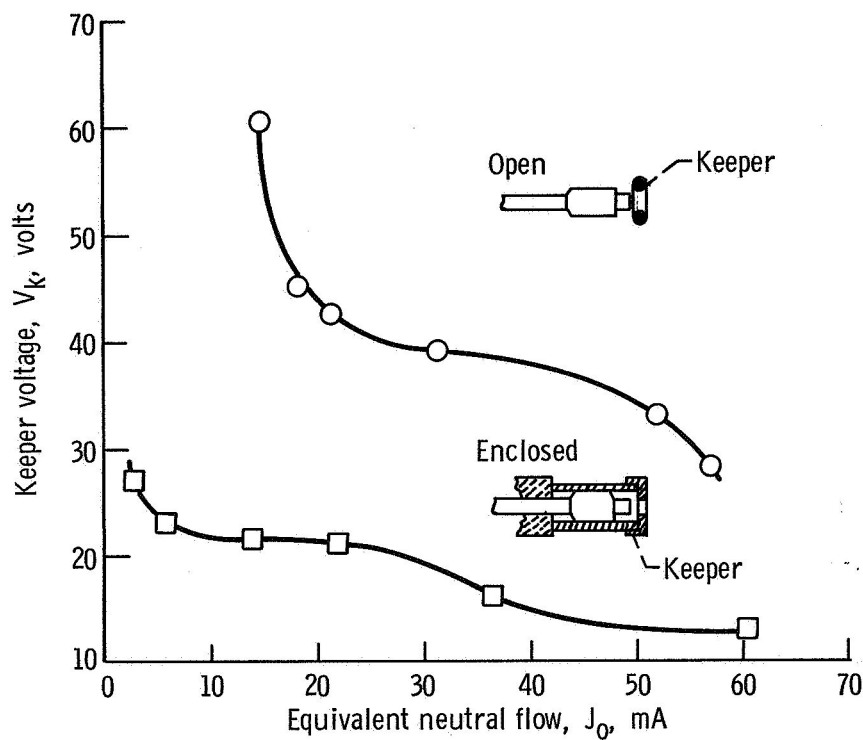


Figure 12. - Performance comparison of two hollow-cathode types operating in 5 cm thruster. Keeper current, 0.5 A. Main discharge off.

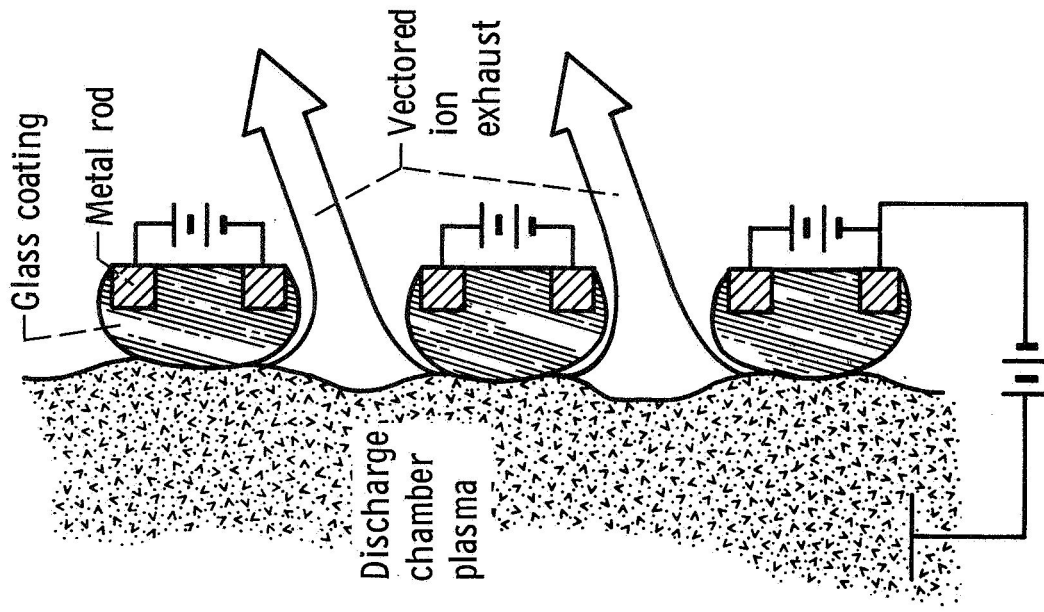
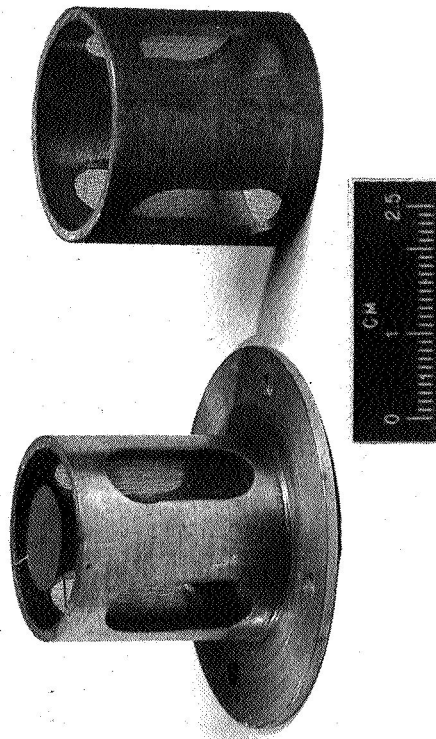


Figure 14. - Portion of a glass-coated accelerator grid with a proposed thrust vectoring method.



C-68-421

Figure 13. - Slotted cathode pole piece and adjustable sleeve. Wire mesh is tantalum.

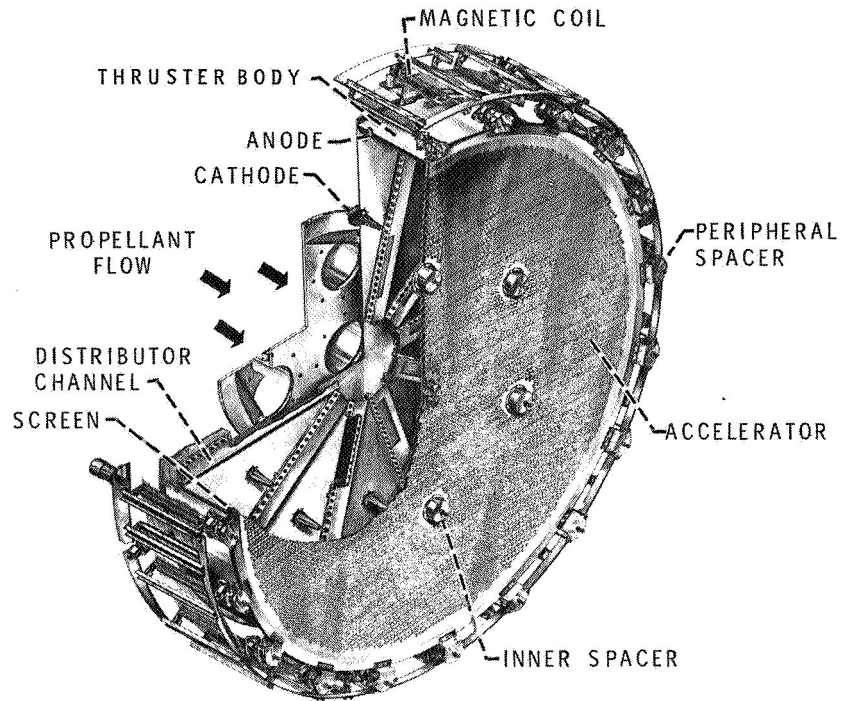


Figure 15. - Cutaway view of 1.5 meter diameter Kaufman thruster.

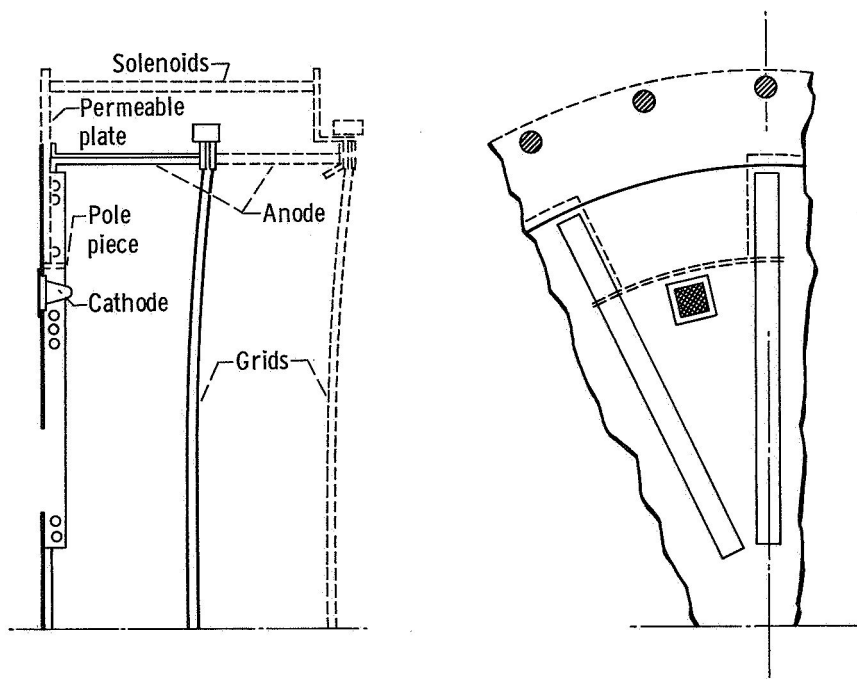
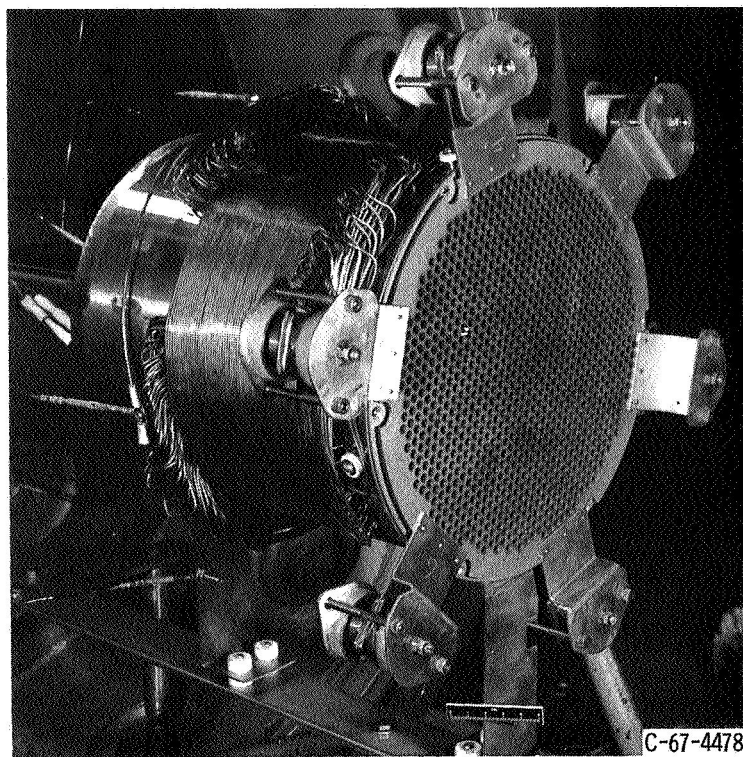
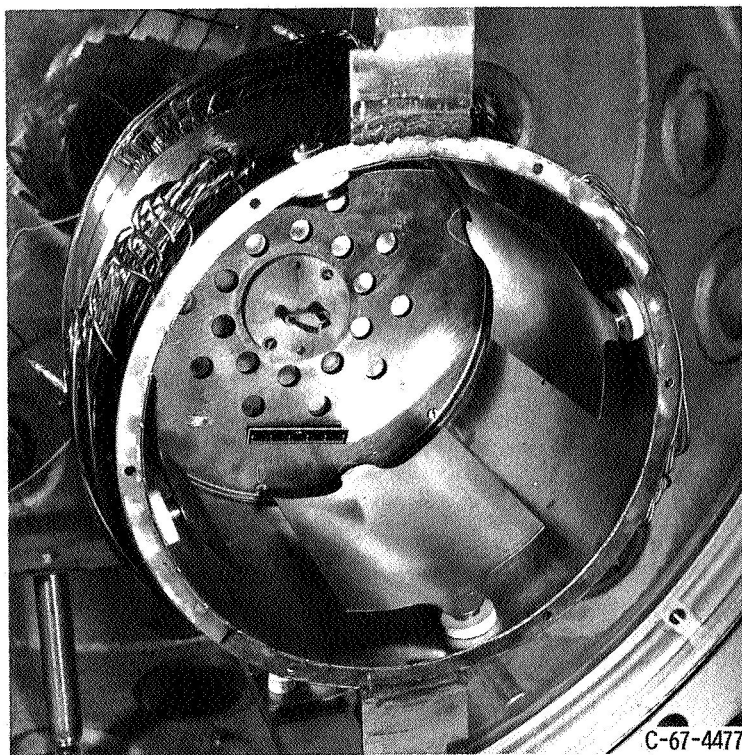


Figure 16. - Section view of 150 cm thruster showing recent modifications (dashed lines).



C-67-4478

(a) Accelerator grids in place.



C-67-4477

(b) Accelerator removed showing segmented anode.

Figure 17. - 20 cm combined-field thruster.

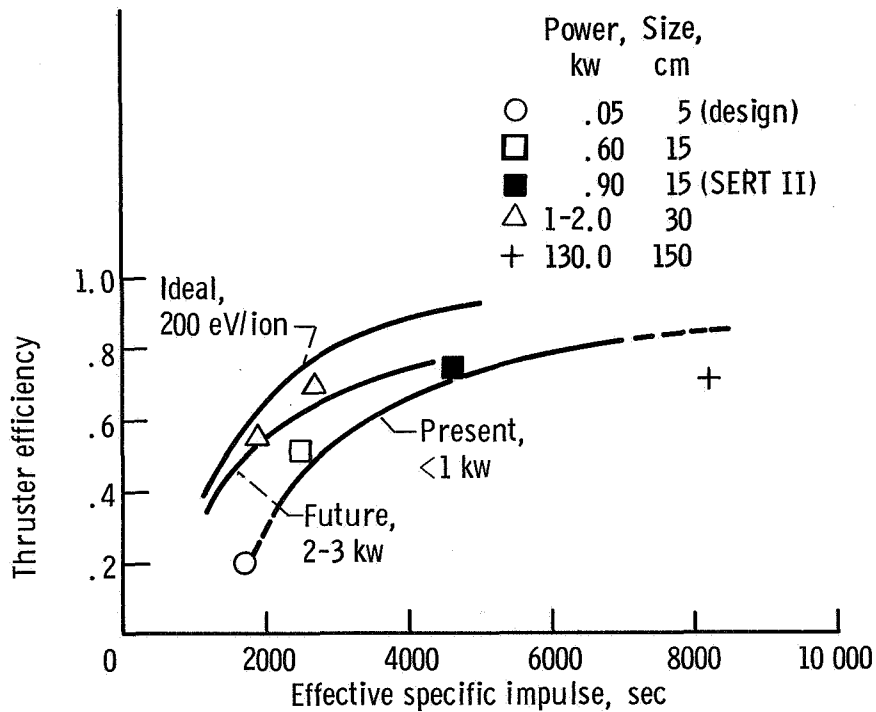


Figure 18. - Comparison of various current Lewis bombardment thrusters. Present and future curves from reference 30. Open symbols for thrusters using glass-coated accelerator.